Can Angular Oscillations Probe Superfluidity in Dipolar Supersolids?

Matthew A. Norcia,[1] Elena Poli,[2] Claudia Politi,[1,2] Lauritz Klaus,[1,2] Thomas Bland,[1,2] Manfred J. Mark,[1,2] Luis Santos,[3] Russell N. Bisset,[2] and Francesca Ferlaino[1,2,*]

[1]*Institut für Quantenoptik und Quanteninformation, Österreichische Akademie der Wissenschaften, Innsbruck 6020, Austria*
[2]*Institut für Experimentalphysik, Universität Innsbruck, Innsbruck 6020, Austria*
[3]*Institut für Theoretische Physik, Leibniz Universität Hannover, 30167 Hannover, Germany*

(Received 17 November 2021; revised 3 March 2022; accepted 6 June 2022; published 22 July 2022)

Angular oscillations can provide a useful probe of the superfluid properties of a system. Such measurements have recently been applied to dipolar supersolids, which exhibit both density modulation and phase coherence, and for which robust probes of superfluidity are particularly interesting. So far, these investigations have been confined to linear droplet arrays, which feature relatively simple excitation spectra, but limited sensitivity to the effects of superfluidity. Here, we explore angular oscillations in systems with 2D structure which, in principle, have greater sensitivity to superfluidity. In both experiment and simulation, we find that the interplay of superfluid and crystalline excitations leads to a frequency of angular oscillations that remains nearly unchanged even when the superfluidity of the system is altered dramatically. This indicates that angular oscillation measurements do not always provide a robust experimental probe of superfluidity with typical experimental protocols.

DOI: 10.1103/PhysRevLett.129.040403

Some of the most distinctive manifestations of superfluidity in ultracold quantum gases relate to their behavior under rotation. These include the presence of quantized vortices [1–3] and persistent currents in ring traps [4], as well as shape-preserving angular oscillations associated with a "scissors" mode [5]. Measurements of the scissors mode frequency have long been used to illuminate the superfluid properties of a variety of systems [6–11]. With the recent advent of dipolar supersolids [12–18]—states that possess both the global phase coherence of a superfluid and the spatial density modulation of a solid—the scissors mode provides a tempting way to quantify changes in superfluidity across the superfluid-supersolid transition [19,20]. Angular oscillations have also been used to search for superfluid properties in solid helium [21]. In this case, however, a change in oscillation frequency initially attributed to superfluidity was eventually traced, instead, to other reasons [22]. In this Letter, we study more deeply the connection between angular oscillations and superfluidity in dipolar supersolids to determine the extent to which such experiments can inform our understanding of superfluidity in these systems.

The goal of these angular oscillation measurements is to infer the flow patterns allowed for a given fluid. A superfluid is constrained by the single-valued nature of its wave function to irrotational flow (IF), while a nonsuperfluid system faces no such constraint and, in certain situations, may be expected to undergo rigid-body rotation (RBR). Prototypical velocity fields for angular oscillations under IF ($\vec{v} \propto \nabla xy$) and RBR ($\vec{v} \propto r\hat{\theta}$) are depicted in Figs. 1(a) and 1(b), respectively. The velocity field associated with angular rotation is related to the moment of inertia of the system and, thus, the frequency of angular oscillations.

The ability to distinguish between RBR and IF (and, thus, in principle, between a classical and superfluid

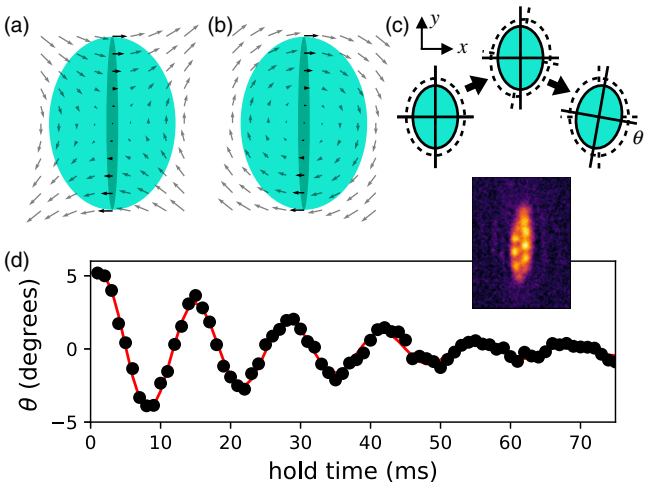

FIG. 1. Characteristic velocity profiles for irrotational flow (a) and rigid-body rotation (b). A wide atomic state (light turquoise oval) samples a region of space where the two differ significantly, while a highly elongated state (dark turquoise oval) samples a region where the two patterns are nearly indistinguishable. (c) We excite oscillations in the angle θ of our atomic gas by rapidly rotating the anisotropic trap (dashed oval), then returning it to its original orientation and observing the subsequent dynamics. (d) Typical example of experimental angular oscillation for the zigzag modulated state shown on the right (image averaged over nine iterations). In this case, the errors from the fit to the state angle are smaller than the markers. The red line is a damped sinusoidal fit used to extract the angular oscillation frequency f_{osc}.

system) depends critically on the geometry of the system, and is sensitive only to the character of the flow pattern where the atomic density is appreciable. As illustrated in Figs. 1(a) and 1(b), highly elongated states sample only the region along the weak axis of the trap (near $x = 0$) where IF and RBR are identical for small rotations (dark turquoise regions), while rounder states (light turquoise regions) sample regions of space where the flow patterns differ significantly and, thus, are far more sensitive to the irrotational constraint. Recent works have focused on systems that form a short linear chain of about two "droplets" [23] in the supersolid regime [19,20].

In this Letter, we study angular oscillations in systems with linear and two-dimensional modulation to disentangle the effect of three important contributions: (i) a narrowing of the aspect ratio of the gas (geometrical change), (ii) a reduction in the population of the low-density superfluid "halo" that occupies the outer regions of the trap, and (iii) a reduction in the density of the interdroplet connection that enables the exchange of atoms between droplets, which is key to the superfluid nature of supersolid systems. We find that, in linear systems, contributions (i) and (ii) dominate the change in oscillation frequency associated with the onset of modulation, while (iii) has a negligible effect.

In dipolar condensates with two-dimensional structure, which have been a focus of recent work [24–28], the effects of geometry and superfluidity may be disentangled, and one may expect to observe a direct link between a change of the superfluid fraction and a modification of the angular oscillation frequency. However, we find that the physics at play is much more complex. Indeed, not only does the oscillation frequency fail to approach its rigid-body value for states with a vanishing superfluid connection, but it remains very close to the value predicted for a superfluid state. We extensively investigate the system behavior as a function of geometry and interaction parameters, revealing a unique multimode response of the dipolar supersolid.

Experimentally, we use a dipolar quantum gas of ^{164}Dy atoms (up to approximately 5×10^4 condensed atoms), confined within an optical dipole trap (ODT) of tunable geometry, formed at the intersection of three laser beams [25,27,29]. The trap geometry and particle number at the end of the evaporative cooling sequence determine the character of the modulated ground state, which can form linear, zigzag, or triangular lattice configurations [28]. By varying the applied magnetic field in the vicinity of Feshbach resonances near 18–23 G, we can access scattering lengths that correspond to either unmodulated BECs or modulated states. In past works, we have demonstrated that modulated states created at the corresponding field have global phase coherence [25,27]. In this Letter, we expect the same to be true, but refer to these experimental states simply as modulated, as we do not repeat the characterization for every trap condition used. We excite angular oscillations by using the well-established protocol of applying a sudden small rotation of the trap, by varying the relative powers in the ODT beams for 6 ms before returning them to their original values [Fig. 1(c)]. Using our high-resolution imaging [30], we observe the in-trap density profile at a variable time from the excitation, and extract the angle of the major and minor axes using a two-dimensional Gaussian fit to the state [31].

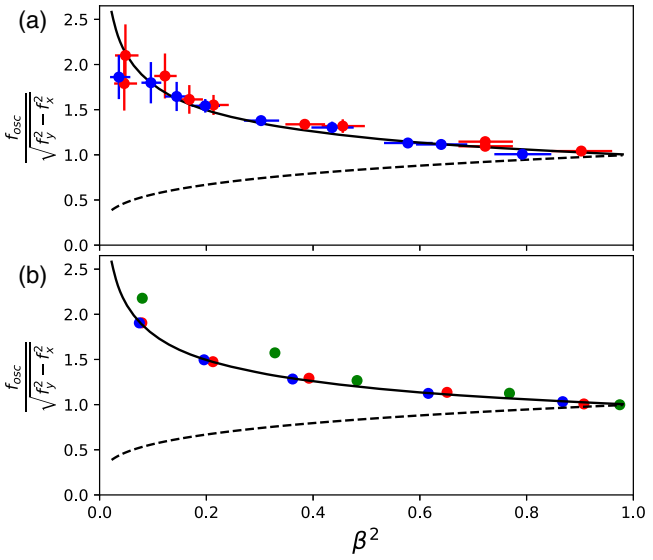

FIG. 2. Normalized oscillation frequencies $f_{\rm osc}$ from experiment (a) and simulation (b). Blue points represent unmodulated BECs, red points represent modulated states (expt.) and supersolid states (sim.), and green points represent independent droplet arrays. Solid lines are predictions for irrotational flow $f_{\rm irr}$. Dashed lines are predictions for rigid body rotation $f_{\rm rig}$. The trap frequencies used in the simulation, from left to right, are $(f_x, f_y) = [(43, 53), (40, 57), (37, 62), (32, 70), (26, 87)]$ Hz. $f_z = 122$ Hz for all cases. A similar range is used in the experiment.

A typical angular oscillation is shown in Fig. 1(d), for a "zigzag" modulated state [25]. From such oscillation traces, we extract the dominant oscillatory frequency $f_{\rm osc}$ using a fit to an exponentially damped sinusoid. Typically, the statistical error on our measurements of $f_{\rm osc}$ is on the sub-Hertz level, better than our knowledge of the trap frequencies, due to drifts between calibrations. We perform such measurements for trap geometries ranging from an elongated cigar shape to pancake shaped, and for different scattering lengths, as summarized in Fig. 2(a).

Within a single-mode approximation, the angular oscillation frequency $f_{\rm osc}$ can be predicted using either a sum-rule based approach [19,34], or considerations based on hydrodynamic flow [5]. For RBR, the angular oscillation frequency is given by $f_{\rm rig} = \sqrt{(f_y^2 - f_x^2)\beta}$, whereas for IF, the predicted value is $f_{\rm irr} = \sqrt{(f_y^2 - f_x^2)/\beta}$ [19,20]. Here, $f_{x,y}$ are the trap frequencies along directions x and y. $\beta = \langle x^2 - y^2 \rangle / \langle x^2 + y^2 \rangle$ is a geometrical factor that quantifies the degree of elongation of the atomic cloud (but carries no

information about the superfluid fraction). As shown in Fig. 2, f_{rig} and f_{rig} are more distinct for smaller values of β. Remarkably, independent of trap geometry or the presence of modulation, we observe f_{osc} close to the IF prediction and far from the RBR prediction when the two predictions differ appreciably.

To gain a deeper understanding of our observations, we theoretically study the oscillation dynamics using a real-time simulation of the extended Gross-Pitaevskii equation (EGPE) [35–37]. To compare to the experimental observations of Fig. 2(a), first, we calculate the ground state for a given trap, scattering length, and atom number. Then, we apply a 0.5° rotation of the trap for 6 ms (we have confirmed that the character and frequency of the response do not change for much larger excitations), and then let the state evolve for 50 ms. Then, we perform the same fitting procedure as used in the experiment to extract f_{osc}. For the simulation, we calculate β directly for the ground state (we confirm that the exact value of β agrees with that extracted from a Gaussian fit at the 5% level). For simulations performed on states ranging from the unmodulated BEC to supersolid (SS) to independent droplet (ID) regimes, with vanishing superfluid connection between droplets, we again find that f_{osc} is always very close to f_{irr}, in very good agreement with the experimental data. For isolated droplet states in particular, f_{osc} can actually be even higher than the expected value for irrotational flow, indicating that the oscillation frequency is not necessarily in between the irrotational and rigid body values.

To further illuminate the dependence f_{osc} on superfluidity, we analyze the results of the simulation as a function of the s-wave scattering length a_s (Fig. 3). Scattering lengths of $85a_0$ yield arrays of (nearly) independent droplets, while $a_s = 97a_0$ produces an unmodulated BEC. In between, we find supersolid states, with low-density connections between droplets. Inspired by the formulation of Leggett [38], we quantify the degree of interdroplet density connection as $\mathcal{C} = [\int dx/\rho(x)]^{-1}$, where $\rho(x)$ is the projected atomic density, evaluated over the interdroplet connection [Fig. 3(a)] [39].

As shown in Fig. 3, despite the rapid reduction of $\mathcal{C}$ with a_s, the simulated f_{osc} exhibits a rather constant behavior with a value always close to the purely irrotational predictions, f_{irr}, for both a linear (1D) and hexagon state (2D). This observation indicates that (i) the degree of interdroplet connection is not actually a major determinant of the angular oscillation frequency and (ii) that the system does not undergo RBR even for vanishingly small interdroplet density connection. The latter conclusion is particularly evident for hexagon states, where the rigid-body prediction substantially departs from the irrotational one. For the linear array, the elongated geometry means that the f_{rig} and f_{irr} differ only slightly; see Supplemental Material for further discussion [31].

At this point, we can clearly see the geometrical limitations of the linear systems. In linear systems, the

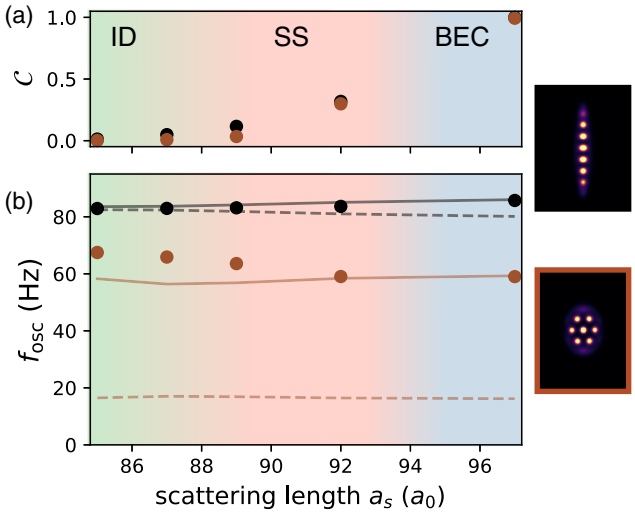

FIG. 3. Impact of scattering length on simulated scissors mode frequencies. (a) Interdroplet connection $\mathcal{C}$ (defined in text) versus scattering length for different trap geometries. The calculated ground state in each trap is shown on the right, with corresponding border colors. (b) Scissors mode frequency versus scattering length. Solid lines are predictions for irrotational flow f_{irr}. Dashed lines are predictions for rigid body rotation f_{rig}. β ranges from 0.93 to 0.99, and 0.27 to 0.31 in the linear and hexagonal cases, respectively.

narrowing of the atomic density distribution that occurs with the onset of modulation causes the dominant contribution to a modification in oscillation frequency as well as a reduction in sensitivity of the oscillation frequency to superfluidity. Simultaneously, the transfer of atoms from the halo to the droplets leads to a reduction of the superfluidity of the composite halo-droplet system, which is accompanied by a small change in the oscillation frequency. However, because the motion induced by rotation in a linear system is perpendicular to the interdroplet axis, these effects should not be interpreted as a result of the weakening superfluid connection along the interdroplet axis. In contrast, systems with two-dimensional structure maintain a relatively round aspect ratio in the modulated regime, and the rotational motion does orient along certain interdroplet axes.

To better understand the nonrigid nature of the angular oscillations, we employ a method to extract the character of the system's response by analyzing our experimental and EGPE simulation dynamics in the frequency domain with respect to time, but in the position domain with respect to the spatial coordinates. A similar technique has been applied along one dimension to understand the mode structure of an elongated condensate [40]. This technique, which for convenience we refer to as "Fourier transform image analysis" (FTIA) [31], allows us to extract a power spectrum of density fluctuations driven by the angular excitation, as well as the spatial form of the density fluctuations at each frequency. For comparison, we also

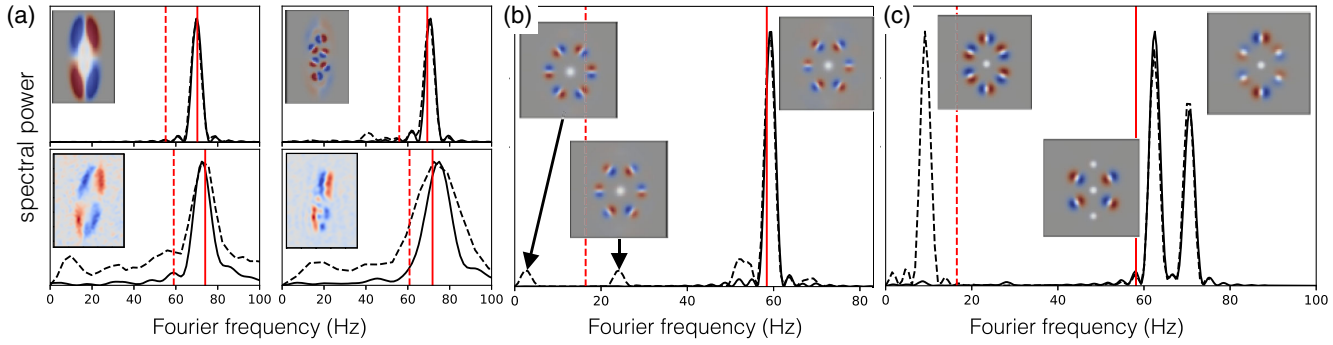

FIG. 4. Analysis of mode shapes and response due to angular excitation. Solid lines are the power spectrum obtained from the rotational signal (θ in the experiment and $\langle xy \rangle$ in the simulation), and dashed lines are obtained from FTIA (see text, Supplemental Material [31] for description). Inset panels show the mode shapes for selected modes. Red and blue indicate out-of-phase changes in density, overlaid onto the average density profile in the panels corresponding to simulation (gray to white). Solid and dashed vertical red lines represent f_{irr} and f_{rig}, respectively. (a) Responses in elongated traps from simulation (top) and experiment (bottom), for an unmodulated BEC (left) and a zigzag droplet state (right). Trap frequencies are $f_{x,y} = [31(1), 73(1), 128(1)]$ Hz, and $f_{x,y,z} = [32, 70, 122]$ Hz for the experiment and theory, respectively. (b) Simulated response of supersolid hexagon state ($a_s = 92a_0$). (c) Simulated response of droplet crystal hexagon state ($a_s = 85a_0$). Note that the ground state has a different orientation for the two scattering lengths in this trap. Trap frequencies are $f_{x,y,z} = [43, 53, 122]$ Hz for (b) and (c).

calculate the spectral power of our rotational signal through a Fourier transform. For computational robustness, we use the fitted angle θ in the experimental case, and $\langle xy \rangle$ for the simulations. To enhance our frequency resolution, we analyze simulations with longer durations than are accessible in the experiment (160 to 290 ms).

We apply the FTIA to both simulation and experimental images in Fig. 4(a). For a BEC, the FTIA gives a dominant peak in both simulation and experiment, whose frequency and shape are consistent with a scissors mode oscillation at the frequency observed from the angular response. For a zigzag modulated state, we again predominantly observe a single peak in the FTIA spectrum at the frequency of the angular oscillation. In the simulation, we can see that the mode corresponds to the motion of the different droplets in a pattern reminiscent of IF in an unmodulated superfluid, and clearly distinct from RBR. In the experiment, the response of individual droplets is not visible due to shot-to-shot fluctuations in the exact number and position of the droplets, but the overall structure is similar to the simulation.

For hexagonal supersolid [Fig. 4(b)] and isolated droplet [Fig. 4(c)] states, the FTIA reveals a clear multifrequency response. For the supersolid, we observe the excitation of modes near 3 and 25 Hz that do not contribute strongly to $\langle xy \rangle$. The droplet motion associated with the 3 Hz mode is approximately (but not exactly) shape preserving, and the frequency is much lower than would be expected for a single-mode RBR response. For the isolated droplet array, we again observe a nearly shape-preserving low-frequency response from FTIA, as well as a dominant angular response that is split into two frequencies, both above the scissors mode frequency f_{irr} expected for a superfluid with the same geometry. In the experiment, the combination of nonangular excitations associated with our method used to rotate the trap and relatively rapid damping of the oscillation prevent us from observing meaningful mode profiles for small β.

Importantly, the FTIA reveals that, even in cases where we observe an apparently single-frequency response in typical rotational observables like θ or $\langle xy \rangle$ [as in Figs. 4(a) and 4(b)], the response of the system may, in fact, be multimode in nature, breaking the single-mode approximation used to analytically extract f_{irr} and f_{rig} [19,34]. In the case of a multifrequency response, f_{irr} and f_{rig}, instead, provide an upper bound for the frequency of the lowest energy excitation—an excitation that is difficult to see with experimentally accessible observables. Features of these subdominant modes, including the lack of a strong rotational signal in the low-frequency oscillations and the apparent similarity between the droplet motion (the motion of the halo is quite different) near 25 Hz to that of the dominant rotational mode, remain interesting topics for future investigation.

As we have noted, not only does the dominant angular response frequency fail to approach the rigid-body value in the isolated droplet regime, but it also stays near to the irrotational prediction. A possible intuitive explanation for this observation is that the flow pattern of Fig. 1(a) resembles that of a quadrupolar surface mode, and it is well known that, for sufficiently strong interactions, the frequency of such modes is predominantly determined by the trap parameters, rather than the details of the interparticle interactions [34].

In conclusion, measurements of angular oscillation frequencies offer a simple way to demonstrate superfluidity in certain conditions. However, care must be taken when making and interpreting such measurements—geometrical

changes can mask the effects of changing superfluidity, and usual predictions to which one might compare rely on the assumption of a single-frequency response of the lowest energy rotational mode. While the moment of inertia of the system is defined as the angular momentum of a system in response to a shape-preserving, steady-state drive, oscillation measurements involve a time-localized change in the rotation rate of the trap, which may excite modes that do not meet this criterion. In small, linear systems, the simple excitation spectra means that approximately shape-preserving oscillations can still be excited [31]. However, we find that a supersolid with 2D structure, which one might expect to be an ideal candidate for such measurements, can exhibit an apparently single-frequency response associated with a mode that is not the lowest in energy. Further, this excitation frequency is typically very close to that of a purely superfluid system, even for systems where the effects of superfluidity are minimal. Therefore, such measurements do not provide a robust indicator of superfluidity for modulated systems. In the future, it may be possible to extract information about superfluidity using a modified excitation scheme to preferentially excite the lower energy modes and a more comprehensive analysis scheme suitable for multifrequency response [41]. However, such techniques would require detailed knowledge of the exact excitation applied and measurement of response amplitudes, both of which are considerably more challenging in an experiment than measuring the frequency of an oscillation.

Finally, we note that, even in the case of single-frequency response, where the frequency of angular oscillations has a direct connection to the moment of inertia of the system, making a clear connection between the moment of inertia and quantities like a superfluid fraction can be problematic. Past works have predicted that a system which is partially superfluid should have a moment of inertia in between the RBR and IF predictions, linearly interpolated according to a superfluid fraction [20,38]. While this interpretation may be valid for systems featuring a rigid crystalline structure and a uniform distribution of crystalline and superfluid components, as in [38], it is not necessarily valid for our small dipolar supersolids, which, in addition to coupled superfluid-crystalline excitations, feature a nonuniform degree of modulation across the system.

We thank Sandro Stringari and Alessio Recati for useful discussions. We acknowledge R. M. W. van Bijnen for developing the code for our EGPE ground-state simulations. The experimental team is financially supported through an ERC Consolidator Grant (RARE, Grant No. 681432), an NFRI grant (MIRARE, Grant No. ÖAW0600) of the Austrian Academy of Science, the QuantERA grant MAQS by the Austrian Science Fund FWF Grant No. I4391-N. L. S. and F. F. acknowledge the DFG/FWF via Grant No. FOR 2247/PI2790. L. S. acknowledges funding by the Deutsche Forschungsgemeinschaft (DFG, German Research Foundation) under Germany's Excellence Strategy—Grant No. EXC-2123 QuantumFrontiers—390837967. M. A. N. has received funding as an ESQ Postdoctoral Fellow from the European Union's Horizon 2020 Research and Innovation Programme under the Marie Skłodowska Curie Grant Agreement No. 801110 and the Austrian Federal Ministry of Education, Science and Research (BMBWF). M. J. M. acknowledges support through an ESQ Discovery Grant by the Austrian Academy of Sciences. We also acknowledge the Innsbruck Laser Core Facility, financed by the Austrian Federal Ministry of Science, Research, and Economy. Part of the computational results presented have been achieved using the HPC infrastructure LEO of the University of Innsbruck.

*Corresponding author.
Francesca.Ferlaino@uibk.ac.at

[1] M. R. Matthews, B. P. Anderson, P. C. Haljan, D. S. Hall, C. E. Wieman, and E. A. Cornell, Vortices in a Bose-Einstein Condensate, Phys. Rev. Lett. **83**, 2498 (1999).
[2] K. W. Madison, F. Chevy, W. Wohlleben, and J. Dalibard, Vortex Formation in a Stirred Bose-Einstein Condensate, Phys. Rev. Lett. **84**, 806 (2000).
[3] M. W. Zwierlein, J. R. Abo-Shaeer, A. Schirotzek, C. H. Schunck, and W. Ketterle, Vortices and superfluidity in a strongly interacting Fermi gas, Nature (London) **435**, 1047 (2005).
[4] A. Ramanathan, K. C. Wright, S. R. Muniz, M. Zelan, W. T. Hill, C. J. Lobb, K. Helmerson, W. D. Phillips, and G. K. Campbell, Superflow in a Toroidal Bose-Einstein Condensate: An Atom Circuit with a Tunable Weak Link, Phys. Rev. Lett. **106**, 130401 (2011).
[5] D. Guéry-Odelin and S. Stringari, Scissors Mode and Superfluidity of a Trapped Bose-Einstein Condensed Gas, Phys. Rev. Lett. **83**, 4452 (1999).
[6] D. Bohle, A. Richter, W. Steffen, A. Dieperink, N. L. Iudice, F. Palumbo, and O. Scholten, New magnetic dipole excitation mode studied in the heavy deformed nucleus ^{156}GD by inelastic electron scattering, Phys. Lett. **137B**, 27 (1984).
[7] O. M. Maragò, S. A. Hopkins, J. Arlt, E. Hodby, G. Hechenblaikner, and C. J. Foot, Observation of the Scissors Mode and Evidence for Superfluidity of a Trapped Bose-Einstein Condensed Gas, Phys. Rev. Lett. **84**, 2056 (2000).
[8] M. J. Wright, S. Riedl, A. Altmeyer, C. Kohstall, E. R. Sanchez Guajardo, J. H. Denschlag, and R. Grimm, Finite-Temperature Collective Dynamics of a Fermi Gas in the BEC-BCS Crossover, Phys. Rev. Lett. **99**, 150403 (2007).
[9] R. M. W. van Bijnen, N. G. Parker, S. J. J. M. F. Kokkelmans, A. M. Martin, and D. H. J. O'Dell, Collective excitation frequencies and stationary states of trapped dipolar Bose-Einstein condensates in the Thomas-Fermi regime, Phys. Rev. A **82**, 033612 (2010).
[10] C. D. Rossi, R. Dubessy, K. Merloti, M. de Goër de Herve, T. Badr, A. Perrin, L. Longchambon, and H. Perrin, The scissors oscillation of a quasi two-dimensional Bose gas as a local signature of superfluidity, J. Phys. Conf. Ser. **793**, 012023 (2017).

[11] I. Ferrier-Barbut, M. Wenzel, F. Böttcher, T. Langen, M. Isoard, S. Stringari, and T. Pfau, Scissors Mode of Dipolar Quantum Droplets of Dysprosium Atoms, Phys. Rev. Lett. **120**, 160402 (2018).
[12] M. Boninsegni and N. V. Prokof'ev, Colloquium: Supersolids: What and where are they?, Rev. Mod. Phys. **84**, 759 (2012).
[13] Z.-K. Lu, Y. Li, D. S. Petrov, and G. V. Shlyapnikov, Stable Dilute Supersolid of Two-Dimensional Dipolar Bosons, Phys. Rev. Lett. **115**, 075303 (2015).
[14] D. Baillie and P. B. Blakie, Droplet Crystal Ground States of a Dipolar Bose Gas, Phys. Rev. Lett. **121**, 195301 (2018).
[15] S. M. Roccuzzo and F. Ancilotto, Supersolid behavior of a dipolar Bose-Einstein condensate confined in a tube, Phys. Rev. A **99**, 041601(R) (2019).
[16] L. Tanzi, E. Lucioni, F. Famà, J. Catani, A. Fioretti, C. Gabbanini, R. N. Bisset, L. Santos, and G. Modugno, Observation of a Dipolar Quantum Gas with Metastable Supersolid Properties, Phys. Rev. Lett. **122**, 130405 (2019).
[17] F. Böttcher, J.-N. Schmidt, M. Wenzel, J. Hertkorn, M. Guo, T. Langen, and T. Pfau, Transient Supersolid Properties in an Array of Dipolar Quantum Droplets, Phys. Rev. X **9**, 011051 (2019).
[18] L. Chomaz, D. Petter, P. Ilzhöfer, G. Natale, A. Trautmann, C. Politi, G. Durastante, R. M. W. van Bijnen, A. Patscheider, M. Sohmen, M. J. Mark, and F. Ferlaino, Long-Lived and Transient Supersolid Behaviors in Dipolar Quantum Gases, Phys. Rev. X **9**, 021012 (2019).
[19] S. M. Roccuzzo, A. Gallemí, A. Recati, and S. Stringari, Rotating a Supersolid Dipolar Gas, Phys. Rev. Lett. **124**, 045702 (2020).
[20] L. Tanzi, J. Maloberti, G. Biagioni, A. Fioretti, C. Gabbanini, and G. Modugno, Evidence of superfluidity in a dipolar supersolid from nonclassical rotational inertia, Science **371**, 1162 (2021).
[21] E. Kim and M. H.-W. Chan, Probable observation of a supersolid helium phase, Nature (London) **427**, 225 (2004).
[22] D. Y. Kim and M. H. W. Chan, Absence of Supersolidity in Solid Helium in Porous Vycor Glass, Phys. Rev. Lett. **109**, 155301 (2012).
[23] Here, the word droplet refers to a high-density region, which is not necessarily self-bound.
[24] J.-N. Schmidt, J. Hertkorn, M. Guo, F. Böttcher, M. Schmidt, K. S. H. Ng, S. D. Graham, T. Langen, M. Zwierlein, and T. Pfau, Roton Excitations in an Oblate Dipolar Quantum Gas, Phys. Rev. Lett. **126**, 193002 (2021).
[25] M. A. Norcia, C. Politi, L. Klaus, E. Poli, M. Sohmen, M. J. Mark, R. Bisset, L. Santos, and F. Ferlaino, Two-dimensional supersolidity in a dipolar quantum gas, Nature (London) **596**, 357 (2021).
[26] J. Hertkorn, J.-N. Schmidt, M. Guo, F. Böttcher, K. S. H. Ng, S. D. Graham, P. Uerlings, H. P. Büchler, T. Langen, M. Zwierlein, and T. Pfau, Supersolidity in Two-Dimensional Trapped Dipolar Droplet Arrays, Phys. Rev. Lett. **127**, 155301 (2021).
[27] T. Bland, E. Poli, C. Politi, L. Klaus, M. A. Norcia, F. Ferlaino, L. Santos, and R. N. Bisset, Two-Dimensional Supersolid Formation in Dipolar Condensates, Phys. Rev. Lett. **128**, 195302 (2022).
[28] E. Poli, T. Bland, C. Politi, L. Klaus, M. A. Norcia, F. Ferlaino, R. N. Bisset, and L. Santos, Maintaining supersolidity in one and two dimensions, Phys. Rev. A **104**, 063307 (2021).
[29] A. Trautmann, P. Ilzhöfer, G. Durastante, C. Politi, M. Sohmen, M. J. Mark, and F. Ferlaino, Dipolar Quantum Mixtures of Erbium and Dysprosium Atoms, Phys. Rev. Lett. **121**, 213601 (2018).
[30] M. Sohmen, C. Politi, L. Klaus, L. Chomaz, M. J. Mark, M. A. Norcia, and F. Ferlaino, Birth, Life, and Death of a Dipolar Supersolid, Phys. Rev. Lett. **126**, 233401 (2021).
[31] See Supplemental Material at http://link.aps.org/supplemental/10.1103/PhysRevLett.129.040403 for more information, which contains refs. [32,33].
[32] I. T. Jolliffe, *Principal Component Analysis*, Springer Series in Statistics (Springer, New York, 2002).
[33] R. Dubessy, C. D. Rossi, T. Badr, L. Longchambon, and H. Perrin, Imaging the collective excitations of an ultracold gas using statistical correlations, New J. Phys. **16**, 122001 (2014).
[34] L. Pitaevskii and S. Stringari, *Bose-Einstein Condensation and Superfluidity* (Oxford University Press, New York, 2016), Vol. 164.
[35] I. Ferrier-Barbut, H. Kadau, M. Schmitt, M. Wenzel, and T. Pfau, Observation of Quantum Droplets in a Strongly Dipolar Bose Gas, Phys. Rev. Lett. **116**, 215301 (2016).
[36] L. Chomaz, S. Baier, D. Petter, M. J. Mark, F. Wächtler, L. Santos, and F. Ferlaino, Quantum-Fluctuation-Driven Crossover from a Dilute Bose-Einstein Condensate to a Macrodroplet in a Dipolar Quantum Fluid, Phys. Rev. X **6**, 041039 (2016).
[37] F. Wächtler and L. Santos, Quantum filaments in dipolar Bose–Einstein condensates, Phys. Rev. A **93**, 061603(R) (2016).
[38] A. J. Leggett, Can a Solid be "Superfluid"?, Phys. Rev. Lett. **25**, 1543 (1970).
[39] We note that the geometry of our system is very different from that considered in Ref. [38], and so, we do not expect this quantity to have a direct connection to the nonclassical moment of inertia of the system. Rather, we simply use it as a convenient way to quantify overlap between droplets.
[40] Edmundo R. Sanchez Guajardo, M. K. Tey, L. A. Sidorenkov, and R. Grimm, Higher-nodal collective modes in a resonantly interacting Fermi gas, Phys. Rev. A **87**, 063601 (2013).
[41] S. M. Roccuzzo, A. Recati, and S. Stringari, Moment of inertia and dynamical rotational response of a supersolid dipolar gas, Phys. Rev. A **105**, 023316 (2022).